

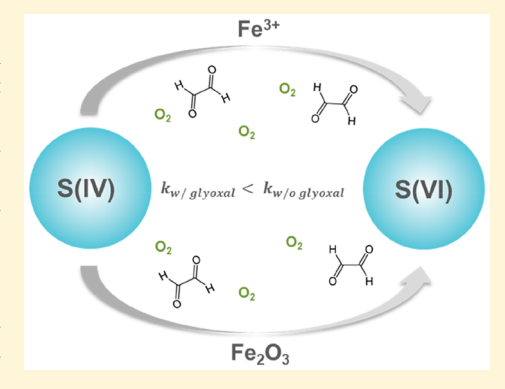
Influence of Glyoxal on the Catalytic Oxidation of S(IV) in Acidic **Aqueous Media**

Ellen M. Coddens,[†] Liubin Huang,[†] Cynthia Wong, and Vicki H. Grassian*®

Department of Chemistry and Biochemistry, University of California San Diego, La Jolla, California 92093, United States

Supporting Information

ABSTRACT: The role of glyoxal in S(IV) oxidation in acidic aqueous solutions catalyzed by iron in the form of aqueous Fe³⁺ ions and solid iron oxide was investigated under different experimental conditions. It is found that the rate of Fe³⁺(aqueous (aq)) ion-catalyzed S(IV) oxidation decreases in the presence of glyoxal. The results of mass spectral analysis and infrared spectra suggest that the trapping of SO₄⁻ radicals, as well as the formation of glyoxal-S(IV) adducts, are responsible for this inhibition effect. Interestingly, although sulfur oxidation is kinetically inhibited in the presence of glyoxal, S(IV) in the form of sulfite is over time completely converted to sulfate. Additionally, the inhibition effects of glyoxal can also be observed in the reaction of S(IV) catalyzed by iron oxide particles, albeit less than that catalyzed by dissolved Fe³⁺(aq). The observed inhibition effect for the iron oxide particles is proposed to be attributed to competitive surface adsorption on the iron oxide particle



surface. Overall, these findings suggest that the effects of glyoxal on the catalytic oxidation of S(IV) are highly dependent on the mechanism, form of iron (dissolved vs solid), and the ambient conditions including pH and concentration.

KEYWORDS: glyoxal, transition metal ions, aqueous reactions, heterogeneous reactions, S(IV) oxidation

1. INTRODUCTION

The aqueous phase oxidation of sulfur dioxide (SO₂) in cloud or fog droplets is considered the most important pathway for the formation of atmospheric sulfate. In fact, it is estimated that 9-17% of the global sulfate production is formed specifically via the oxidation of aqueous SO₂ in the presence of transition-metal ions (TMI), for example, iron and manganese.2

Earlier studies have shown that the catalytic oxidation of S(IV) by TMI is a complex process for which its mechanisms and kinetics are dependent on reaction conditions including pH, temperature, and light.3 Furthermore, recent studies have shown that this reaction can also be influenced by other reactions, in particular, in the presence of organic compounds. For example, it has been established that some organic acids, such as oxalic acid and formic acid, have a strong inhibition effect on iron-catalyzed S(IV) oxidation due to the complexation of organic ligands with iron. 4-6 The catalytic oxidation of S(IV) is a free-radical chain reaction, 3,7,8 where sulfoxy radicals, that is, SO₃-, SO₄-, and SO₅- radicals, are the major intermediates. Therefore, besides complexation with TMI, organic compounds can also react with sulfoxy radicals, resulting in the decrease of sulfoxy radical concentration and subsequently altering the rate of catalytic S(IV) oxidation as well as the conversion of S(IV). The three main pathways for these reactions in aqueous phase are summarized in reactions R1-R3 (using SO₄⁻ radical as an example): ^{17,1}

$$\cdot SO_4^- + HR \rightarrow HSO_4^- + \cdot R \tag{R1}$$

$$\cdot SO_4^- + C_6H_6 \rightarrow C_6H_6^+ + SO_4^{2-}$$
 (R2)

$$\cdot SO_4^- + H_2C = CHR \rightarrow -S(O)_2OCH_2 - CHR$$
 (R3)

Specifically, the ·SO₄ radical can react with saturated organic compounds through hydrogen abstraction (R1), transfer of an electron from an aromatic compound (R2), and undergo addition reactions with organic compounds containing carbon-carbon double bonds (R3). Despite the fact that it is known that organic compounds can impact the catalytic oxidation of S(IV), $^{4-6,11-16}$ the understanding of how this occurs for carbonyl compounds, which are important species involved in atmospheric chemistry with some having large apparent Henry's law constants (e.g, carbonyl compounds including formaldehyde, glyoxal, and acetone), 19 is still limited. Furthermore, in addition to aqueous metal ions, previous studies have shown that S(IV) can also be oxidized by transition metal-containing particles in the aqueous phase through homogeneous as well as heterogeneous reactions,² indicating that the mechanism by which S(IV) reacts with these particle inclusions is different than that with TMI. However, very little is known about the process of S(IV) oxidation by mineral dust particles in the presence of organic compounds in the aqueous phase.

October 30, 2018 Received: Revised: December 3, 2018 Accepted: December 4, 2018

Published: December 4, 2018

Glyoxal, the simplest α -dicarbonyl compound, is produced from the oxidation of biogenic and anthropogenic volatile organic compounds (VOCs), including isoprene, terpenes, and aromatic hydrocarbons.^{27–30} Because of its high solubility (effective Henry's law constant of $(3.0-4.2) \times 10^5 \,\mathrm{M} \,\mathrm{atm}^{-1}$ at 25 °C), ³¹ glyoxal easily partitions into the aqueous phase and is found widely in atmospheric aerosols, clouds, and fog droplets, 32 making it an important contributor to the formation of aqueous secondary organic aerosols (SOA) and a source of other water-soluble products. ^{33–38} Given its prevalence and importance in the atmosphere, glyoxal was selected to investigate the impact it has on the catalytic oxidation of S(IV). In particular, we investigated the aqueous-phase reaction of S(IV) catalyzed by iron (Fe³⁺(aqueous (aq)) and Fe_2O_3) in the presence and absence of glyoxal. The purpose of this study is to determine the effect of glyoxal on the kinetics of this process under various atmospherically relevant conditions and relevant possible mechanisms.

2. MATERIALS AND METHODS

2.1. Reagents and Materials. Aqueous S(IV) solutions were prepared from Na₂SO₃(LabChem) and Na₂S₂O₅ (>97%, Alfa Aesar). FeCl₃ (98%, Alfa Aesar) and Fe₂(SO₄)₃ (Sigma-Aldrich) were used as the source of aqueous Fe(III) for kinetic studies and mechanism studies, respectively. Iron oxide (γ-Fe₂O₃, 99%, Alfa Aesar) was used as the source of solid Fe(III). The characterization of iron oxide is described in detail in our previous study. ²⁶ Briefly, the Brunauer–Emmett–Teller (BET) surface area of γ-Fe₂O₃ was measured as 56 ± 1 m² g⁻¹. Solutions were prepared with Na₂SO₃/Na₂S₂O₅, glyoxal (Acros, 40 wt %), and Fe(III) diluted in ultrapure water (Milli-pore). Oxygen was dissolved in water by equilibration with air. The initial pH of the solution was adjusted to 5.0 or 3.0 by HCl (1 M, Fisher)/H₂SO₄ (1 M, Fluka).

2.2. Aqueous-Phase Reactor. To investigate the role of glyoxal in the reaction of S(IV) in the form of sulfite/bisulfite solutions catalyzed by iron, kinetic studies of aqueous-phase reactions were conducted in a 0.1 L water-jacketed quartz vessel. A solution of 0.1 mM Na₂S₂O₅ mixed with different glyoxal concentrations (0–0.5 mM) and FeCl₃ (\sim 8 μ M) or γ - Fe_2O_3 (0.1 g L⁻¹) was introduced into the reactor for a total volume of 75 mL. The remaining space was maintained over the liquid level for mixing. The details of the experimental conditions are listed in Table S1. For all experiments, reactors were continuously stirred, and the temperature was controlled to 25 °C in the dark. Aliquots of the reaction mixture were extracted every 3 or 5 min for the duration of 18 or 30 min. After reaction, 75 µL of formaldehyde (CH2O, 0.1 M) were added to each sample to prevent further oxidation. In the experiments with iron oxide, samples were filtered with a 0.2 μ m polytetrafluoroethylene (PTFE) filter to remove solid particles before adding HCHO. After reaction, samples were analyzed with ion chromatography to obtain accurate sulfite concentrations. Selected samples were analyzed to monitor S(IV) oxidation using attenuated total reflectance-Fourier transform infrared (ATR-FTIR) spectroscopy. However, for these studies, initial concentrations of reagents (S(IV) (50 mM), glyoxal (50 mM), and γ -Fe₂O₃ (1 g L^{-1})) were used.

In addition to investigating the kinetics of these reactions, we also performed experiments to explore the mechanism of the reactions. The products from Na_2SO_3 reacted with $Fe_2(SO_4)_3$ in the presence and absence of glyoxal were

investigated using a 20 mL glass reactor. The sample preparation for these experiments is described in detail elsewhere. The initial concentrations of Na_2SO_3 , glyoxal, and Fe^{3+} (aq) were 2, 2, and 0.25 mM, respectively. The highly concentrated solution was used to facilitate the characterization of reaction products. All experiments were performed at 277 K under dark conditions for ~ 12 h of reaction time, and products were analyzed with a high-resolution hybrid linear ion trap mass spectrometer equipped with a heated electrospray ionization (HESI) source (HESI-HRMS, Thermo Orbitrap Elite).

2.3. Detection of Reactants and Products. 2.3.1. The Measurement of S(IV) and S(VI) Concentration. The concentrations of S(IV) and S(VI) were determined by ion chromatography (IC, Dionex ICS2000) equipped with a Dionex AS25 analytical column, which allowed peaks for sulfite and sulfate to be completely separated under the following gradient program: the concentration of eluent (KOH, Thermo Scientific) increased from 15 to 36 mM at 0–20 min, held at 36 mM for 10 min, and then decreased to 10 mM from 30 to 35 min. During each run, the eluent flow rate was maintained at 0.25 mL min⁻¹ with a column temperature of 30 °C. For each analysis 25 μ L of sample was injected.

As noted above, CH2O was added to each sample immediately after solution extraction; thus, the unreacted S(IV) can be combined with CH₂O to form hydroxymethanesulfonate (HMS). Control experiments revealed that the addition of CH₂O does not interfere with the determination of S(IV) concentration in this study. Additionally, given that some residual S(IV) may be in the form of glyoxal-S(IV)adducts, we also evaluated the influence of different aldehyde-S(IV) adducts for the measurement of sulfite concentration by comparing the retention time and intensity of the S(IV) peak in the form of glyoxal-S(IV) adducts with that in the form of formaldehyde-S(IV) adducts. The results showed that the different form of aldehyde-S(IV) adducts does not induce a discrepancy of S(IV) measurement. Furthermore, we also determined the stability of the sample, finding that the intensity of the sample did not change within 48 h. To avoid interferences, we measured the samples immediately after reaction.

2.3.2. Products Analysis. Samples obtained from the experiments for mechanism studies were analyzed by HESI-HRMS under negative ionization mode. Samples were diluted by a factor of 20 with acetonitrile (ACN, Fluka) before analysis. The details of this method can be found in our previous work.³⁹

ATR-FTIR spectroscopy measurements of sulfur oxidation were taken using a Thermo-Nicolet spectrometer equipped with an MCT/A detector. A background spectrum was collected of water (Milli-Q) on the blank Ge crystal in a horizontal ATR cell (Pike Technologies, Inc.). Solution-phase spectra were recorded for each aliquot extracted during dissolution experiments by depositing $\sim\!\!1$ mL of each filtered aqueous sample onto the ATR crystal. A total of 200 scans were acquired at 4 cm $^{-1}$ resolution for each spectrum.

2.3.3. Measured Dissolved Iron Concentrations. Selected samples were analyzed with inductively coupled plasma-mass spectrometry (ICP-MS) (iCAP RQ ICPMS, Thermo Fisher Scientific) to determine total iron concentration. A 100 ppm Fe standard for ICP-MS (Inorganic Ventures) was diluted to concentrations of 1, 0.1, 0.01, 0.001, 0.0001, and 0.000 01 ppm

to generate a calibration curve. Samples were acidified using nitric acid, and ICP-MS internal standard (Inorganic Ventures) was added to each sample. The average and standard deviation are reported for all dissolution measurements.

3. RESULTS AND DISCUSSION

3.1. S(IV) Oxidation with Fe(III) in the Aqueous Phase. Kinetic studies of S(IV) oxidized by Fe³⁺(aq) in the absence and presence of glyoxal at pH 5 were investigated. Figure 1

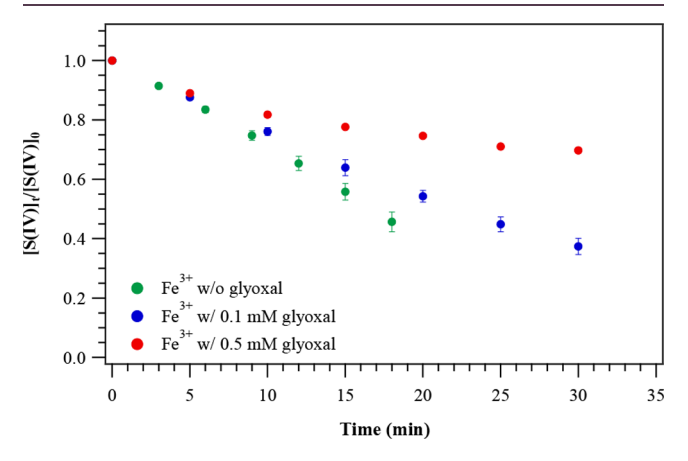


Figure 1. Effect of glyoxal on Fe³⁺-catalyzed S(IV) oxidation at pH 5. Experimental conditions: $[S(IV)]_0 = 0.18$ mM; [glyoxal] = 0-0.5 mM; $[Fe^{3+}] = 8 \mu M$; T = 25 °C.

shows the time dependence of $[S(IV)]_t/[S(IV)]_0$ ratio, where $[S(IV)]_t$ is the concentration of S(IV) at time t, and $[S(IV)]_0$ is the initial concentration of S(IV). The experimental data show that the reaction is zero order with respect to S(IV) in the presence of $Fe^{3+}(aq)$ alone as well as in the simultaneous presence of $Fe^{3+}(aq)$ and glyoxal. Therefore, the reaction rate is described by E1:

$$-\frac{\mathrm{d}[\mathrm{S}(\mathrm{IV})]}{\mathrm{d}t} = k \tag{E1}$$

where k is the observed rate constant calculated from at least two repeated experiments. As shown in Table 1, in the

Table 1. Observed Rate Constants, k, for the Catalytic Oxidation of S(IV) in the Presence and Absence of Glyoxal

	[glyoxal] (mM)	$k \text{ (mM s}^{-1})$	$k (s^{-1})$
		pH 5	pH 3
Fe ³⁺	0	$9.1 \pm 0.5 \times 10^{-5}$	$6.0 \pm 0.3 \times 10^{-3}$
	0.1	$6.3 \pm 0.3 \times 10^{-5}$	$2.4 \pm 0.1 \times 10^{-3}$
	0.5	$2.9 \pm 0.1 \times 10^{-5}$	$1.4 \pm 0.1 \times 10^{-3}$
γ -Fe ₂ O ₃	0	$4.6 \pm 0.1 \times 10^{-5}$	$3.7 \pm 0.2 \times 10^{-3}$
	0.1	$3.5 \pm 0.1 \times 10^{-5}$	$2.8 \pm 0.1 \times 10^{-3}$

presence of Fe³⁺(aq) only, the value of k is measured as $(9.1 \pm 0.5) \times 10^{-5}$ mM s⁻¹. Even though considering the contribution of S(IV) oxidized by O₂ (Figure S1), this value is still calculated to be $(7.7 \pm 0.5) \times 10^{-5}$ mM s⁻¹, indicating that Fe³⁺ plays an important role in the S(IV) oxidation. However, in the presence of 0.1 mM glyoxal, the value of k decreases to $(6.3 \pm 0.3) \times 10^{-5}$ mM s⁻¹, suggesting that glyoxal inhibits the reaction. It is expected that this inhibition effect is closely related to the glyoxal concentration. Increasing the glyoxal

concentration from 0.1 mM to 0.5 mM resulted in a decrease of the rate by \sim 54%.

Solution pH is a major factor in the catalytic oxidation of S(IV), which can affect the mechanism and rate of reaction by controlling the distribution of both S(IV) and metal ion species and altering the stability of the produced metal—sulfur complexes.³ Thus, the effect of glyoxal on this catalytic reaction at different pH was investigated. Analogously, the change of $[S(IV)]_t/[S(IV)]_0$ ratio as the function of time is depicted in Figure 2. It can be seen that the rate of S(IV) loss at pH 3 is

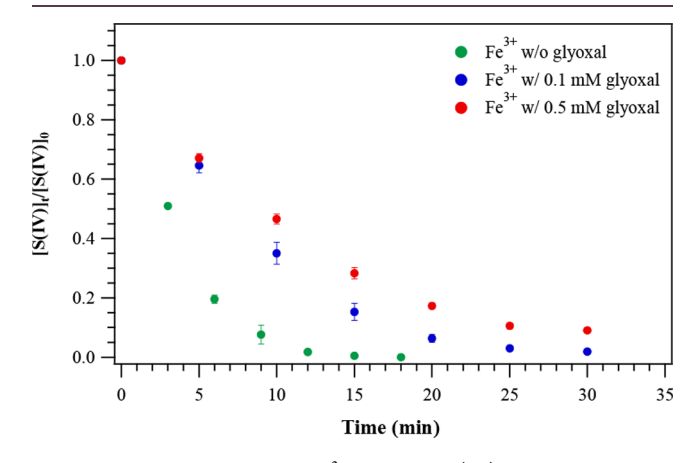


Figure 2. Effect of glyoxal on Fe³⁺-catalyzed S(IV) oxidation at pH 3. Experimental conditions: $[S(IV)]_0 = 0.16$ mM; [glyoxal] = 0-0.5 mM; $[Fe^{3+}] = 8$ μ M; T = 25 °C.

much faster than that at pH 5, and the reaction order with respect to S(IV) changes to approximate first order (Figure S2). The change of reaction order at different pH values has been previously reported.³ In the presence of Fe³⁺(aq) only, the rate constant k was calculated to be $(6.0 \pm 0.3) \times 10^{-3} \text{ s}^{-1}$ (Table 1). Similar to pH 5, we also find the rate constant to have a negative dependence on glyoxal concentration at pH 3. To estimate the magnitude of the inhibition effect of glyoxal on this reaction, the ratio of k/k', where k' is the observed rate constant in the presence of glyoxal, was determined. At pH 3, the value of the ratio of k/k' is 2.5, which is higher than that at pH 5 (k/k' = 1.4), suggesting that the inhibition effect of glyoxal is more pronounced at pH 3; the possible explanations are discussed below. Interestingly, as shown in Figure 2, the remaining S(IV) is barely detected after 30 min of reaction, even in the presence of glyoxal. We calculated the sulfur balance, that is, the measured concentration of S(IV) added with SO₄²⁻, during the reaction. Figure 3 shows a decrease in S(IV) concentration with a concomitant increase of SO₄²⁻ concentration. The value of the sulfur balance after reaction is nearly identical to that in the beginning, suggesting that almost all of the S(IV) is converted to sulfate. This observation agrees with mass spectral data that show that other organosulfur compounds are not observed, except adducts, during this process (Figure 4). This result indicates that, although the presence of glyoxal can slow the oxidation of S(IV) by Fe³⁺, S(IV) is ultimately oxidized to S(VI) over time.

Based on the experimental and literature results, the possible mechanisms for explaining the inhibition effect of glyoxal on the Fe³⁺-catalyzed S(IV) oxidation were elucidated. Schaefer et al. ⁴⁰ measured the rate constant for the reaction of the SO_4^- radical with glyoxal as 2.4×10^7 L mol $^{-1}$ s $^{-1}$, indicating that SO_4^- radicals can also abstract a H atom of glyoxal like OH

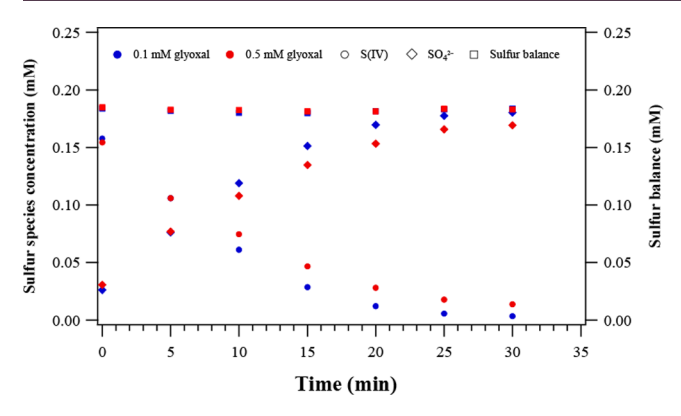


Figure 3. Sulfur balance during the oxidation of S(IV) to S(VI) (SO_4^{2-}) by $Fe^{3+}(aq)$ in the presence of 0.1 and 0.5 mM glyoxal at pH 3.

radicals. They suggested that this value is comparable with those of other mono- and polyfunctional alcohols. 41 However, previous study reported that the hydrogen abstraction by the SO₃⁻ radical can be negligible for alcohol.⁴² Therefore, although the SO₃⁻ radical is the primary radical formed in the catalytic reaction, the reaction of glyoxal with SO₃⁻ radicals is not considered to be important here. If alcohol inhibits the reaction via trapping $\mathrm{SO_4}^-$ radicals, 14 glyoxal may undergo a similar mechanism. The main products generated through this pathway are glyoxylic acid and oxalic acid assuming that the mechanism of H atom abstraction by SO_4^- radicals is analogous to that of OH radicals in aqueous phase reaction.⁴⁰ Figure 4 shows the negative-ion mass spectra of glyoxal reacted with S(IV) in the absence and presence of $Fe^{3+}(aq)$ at pH 5. The peak at m/z 154.97 corresponding to the structure of C₂H₃SO₆ was observed, which is produced from the reversible reaction of HSO₃⁻ with glyoxylic acid that has been previously proposed. 43 The observation of the formation of glyoxylic acid demonstrates that the inhibition effect of glyoxal can contribute to some of the consumption of the SO₄⁻ radicals. The more convincing evidence is that this peak does not exist in the absence of Fe³⁺(aq). However, the peak of another major product, oxalic acid, is not observed in the mass spectra. This may be attributed to oxalate formation and oxalate complexation with iron during the reaction. It is worth noting that the formation of oxalate will reduce the concentration of Fe³⁺(aq), thereby affecting the catalytic oxidation as well.

Because of its high solubility, glyoxal can react with S(IV) to form aldehyde-S(IV) adducts in the aqueous phase. In this study, the formation of glyoxal—S(IV) adducts was verified using ATR-FTIR. Figure S3 shows the IR spectra of the sulfite solution and the sulfite solution mixed with glyoxal. In the spectra of sulfite mixed with glyoxal the band at 1023 cm⁻¹,

which is assigned to the stretching mode of bisulfite, disappears, while a new band appears at $1032~{\rm cm}^{-1}.^{44,45}$ Kaun et al. ⁴⁶ reported that one of the characteristic IR peaks of the HCHO–S(IV) adduct is at $1037~{\rm cm}^{-1}$. Thus, the band at $1032~{\rm cm}^{-1}$ observed in this study is assigned to hydroxyalkylsulfonate. The mechanism for glyoxal–S(IV) adducts formation under acidic conditions has been proposed previously. Here, the simplified mechanism is shown in reactions R4–R7:

$$CHOCHO + H_2O \rightleftharpoons CH(OH)_2CHO$$
 (R4)

$$CH(OH)_2CHO + H_2O \rightleftharpoons (CH(OH)_2)_2$$
 (R5)

$$CHOCHO + HSO_3^- \rightleftharpoons CHOCH(OH)SO_3^-$$
 (R6)

$$CHOCHO + 2HSO_3^- \rightleftharpoons (CH(OH)SO_3^-)_2$$
 (R7)

Since the formation of the dihydrate (R5) is an extremely favorable process for the hydration of glyoxal in aqueous phase, 48,49 the glyoxal-monobisulfite adduct, as well as the glyoxal-dibisulfite adduct, can be formed during the process of adduct formation. As shown in Figure 4, the observed peaks at m/z 138.97 (C₂H₃O₅S) and 156.98 (C₂H₅O₆S) verify the existence of these two species. Interestingly, in addition to the monomer adducts, the peaks at m/z 196.97 and 214.99 correspond to the structures of C₄H₅O₇S and C₄H₇O₈S, respectively, indicating the formation of dimer adducts that have not been reported previously. Given that glyoxal can undergo oligomerization in the aqueous phase, particularly under acidic conditions, 50,51 it is expected that the mechanism for the formation of dimer adducts may be similar to monomer adducts. Previous studies revealed that the formation of adducts cannot appreciably react directly with some oxidants, such as O₂, H₂O₂, and O₃, once formed. 52 Thus, in addition to trapping SO₄ radicals, this nonradical reaction may be responsible for the inhibition of S(IV) catalytic oxidation as well.

To investigate the contribution of these two mechanisms, we performed control experiments under the same experimental conditions with the exception of the initial S(IV) concentration at pH 3. The concentration of S(IV) was adjusted to 2 mM, which is 10 times larger than that used before. If the inhibition effect is mainly induced by reacting with SO_4^- radicals, a significant inhibition effect should still be observed, since the protected S(IV) only accounts for less than 10% of the total S(IV). However, the rate of S(IV) loss in the absence of glyoxal is only 1.1 times larger than that in the presence of glyoxal, indicating that the inhibition effect is dominated by the formation of glyoxal–S(IV) adducts. Furthermore, these results also reveal that this inhibition effect is closely related to the ratio of S(IV) to glyoxal in the solution. If the

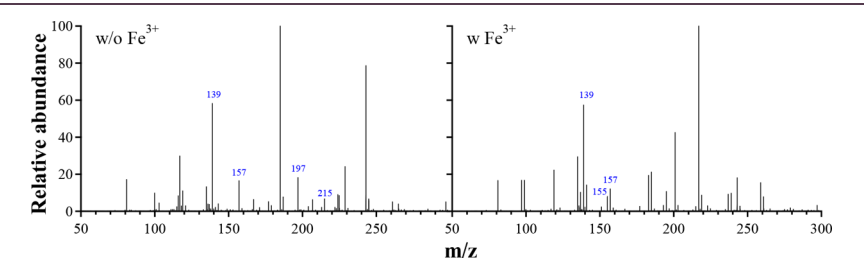


Figure 4. Mass spectra of glyoxal reacted with Na_2SO_3 in the absence and presence of $Fe^{3+}(aq)$ at pH 5. Several peaks are highlighted in blue due to the presence of adducts (see text for further details).

concentration of glyoxal is comparable to S(IV), the presence of glyoxal can significantly affect the oxidation of S(IV); however, if the concentration of S(IV) is excessive, the presence of glyoxal will have a weaker impact on this catalytic reaction.

It is worth noting that the trapping of SO_4^- radicals and the formation of adducts explains the significant decrease in the loss of S(IV) with increasing glyoxal concentration. The higher concentration of glyoxal can accelerate the hydrogen abstraction as well as the formation of glyoxal-S(IV) adducts resulting in the enhancement of the inhibition effect. However, the inhibition effect is significantly enhanced with decreasing pH, which cannot be explained by the mechanism mentioned hereinbefore. Schaefer et al. 40 found that the rate SO₄ radicals reacted with glyoxal is pH-independent. Thus, the discrepancy of the inhibition effect between pH 3 and pH 5 may not be related to the mechanism of trapping SO₄⁻ radicals. Additionally, Olson and Hoffmann⁴⁷ investigated the kinetics of glyoxal-S(IV) adducts formation as a function of pH and found that the rate of adduct formation increases with increasing pH, but the dissociation of these adducts is also positively pH dependent. Although they have not investigated the adduct stability constants of glyoxal adducts as a function of pH, they suggested that this constant should be independent over the range of pH 3-5, since the form of adducts, S(IV), and glyoxal species remain the same in this pH range. However, the major assumption of their inference is that the glyoxal adduct contains two monomer structures, that is, glyoxal-monobisulfite and glyoxal-dibisulfite. In this study, we point out the existence of dimer adducts and find that the intensity of C₄H₅O₇S peak at pH 3 is twice as large compared to that at pH 5 suggesting that dimer adducts may be easily formed at lower pH. The dimer adducts formed may be more stable than monoadducts; thus, we speculate that the more pronounced inhibition effect at more acidic conditions results from the higher amount of dimer adducts formed. Further studies should be performed to verify this speculation.

3.2. S(IV) Oxidation in Solid-Phase Fe(III). In addition to aqueous Fe(III), previous studies have also shown that the oxidation of S(IV) can be driven by aqueous suspensions of solid catalysts, such as iron oxide. Therefore, in this study, we also investigated the influence of glyoxal on S(IV) oxidation by solid Fe(III), that is, γ -Fe₂O₃. Figure 5 shows the

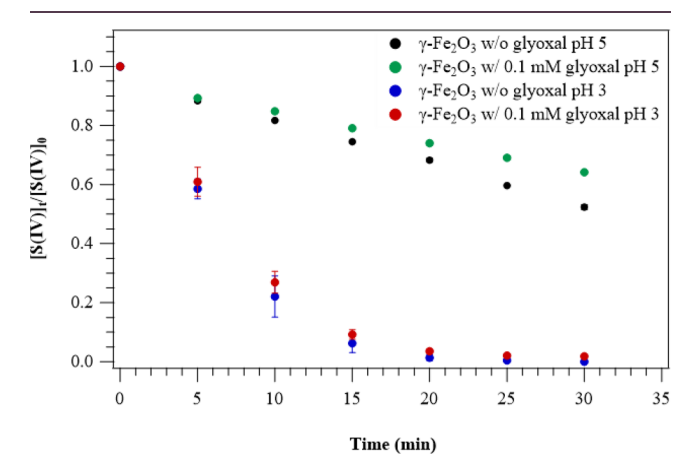


Figure 5. Effect of glyoxal on the reaction of S(IV) with γ -Fe₂O₃ particles. Experimental conditions: [S(IV)]₀ \approx 0.16 mM; [glyoxal] = 0.1 mM; γ -Fe₂O₃ = 0.1 g L⁻¹; T = 25 °C.

change of $[S(IV)]_t/[S(IV)]_0$ ratio over time for the reaction of S(IV) with γ -Fe₂O₃ particles in the presence and absence of glyoxal at different pH values. The rates of reaction are summarized in Table 1. At pH 5, the rate constant in the absence of glyoxal was measured as $(4.6 \pm 0.1) \times 10^{-5}$ mM s⁻¹, which is 1.3 times larger than in the presence of 0.1 mM glyoxal. Interestingly, at pH 3, in contrast to Fe³⁺(aq), the extent of the inhibition effect significantly decreased, where the reaction is only slightly influenced by the presence of glyoxal (Figure 5), suggesting that the mechanism of S(IV) oxidation may be quite different. Note that, under acidic conditions, iron can be leached from particles and then participate in homogeneous catalytic reactions. ^{20,53,54} Thus, the contribution of heterogeneous reaction to the overall S(IV) oxidation is evaluated. We employed ICP-MS to measure the concentration of total dissolved iron ($Fe^{3+} + Fe^{2+}$), which showed that at pH 5 the concentration of dissolved Fe is estimated to be less than 0.01 μ M, meaning that there is little dissolved Fe³⁺ to participate in the oxidation of S(IV). However, the rate constant of S(IV) reacted with γ -Fe₂O₃ particles is 3.5 times higher than that with oxygen only (Figure S1); hence, we infer that the oxidation of S(IV) is dominated by heterogeneous surface reaction. At pH 3, the concentration of dissolved iron is 2 orders of magnitude larger than at pH 5, which is attributed to increased proton promoted dissolution, but the measured concentration of dissolved iron is still less than 1 μ M, and the loss of S(IV) is also much higher than that with oxygen only (Figure S1). Furthermore, the observed weak inhibition effect in the presence of glyoxal is not in agreement with the homogeneous catalytic reaction discussed above. Therefore, the heterogeneous catalysis may also contribute to the loss of S(IV) at pH 3.

Since the oxidation of S(IV) is dominated by the heterogeneous reaction, the mechanism for observed inhibition effect here seems to be different to that observed for aqueous Fe(III). The possible explanation for this is as follows. It is well-known that surface hydroxyl groups are the principal reactive sites on metal oxides surfaces and participate in the conversion of S(IV) to S(VI) on the surface of Fe_2O_3 particles. As noted previously, glyoxal and S(IV) can form glyoxal-S(IV) adducts to resist the oxidization by some oxidants (e.g., H_2O_2 and O_3), but it can be oxidized by aqueous OH radicals producing glyoxal and SO₃⁻ radicals. SS According to the results of formaldehyde-S(IV) adducts investigated by previous studies, 56,57 the rate of glyoxal-S(IV) adducts reacted with OH radicals may be lower than that of HSO₃⁻ reacted with OH radicals.⁵⁸ Thus, the different reactivity of HSO₃⁻ and glyoxal-S(IV) adducts toward surface hydroxyl groups can potentially induce the different rates of S(IV) loss. Another possible explanation is competition between S(IV) and glyoxal for adsorption and reaction with hydroxyl groups. Faust et al.²¹ suggested that the number density of surface hydroxyl groups on α -Fe₂O₃ particles is 9 nm⁻². Assuming that the density of surface hydroxyl groups on these iron oxide particles is of the same order, the amount of surface hydroxyl groups is estimated to be $\sim 4 \times 10^{18}$, and the amount of S(IV) and glyoxal in solution is $\sim 7 \times 10^{18}$ and 4.5 \times 10¹⁸, respectively. Although the heterogeneous reaction of glyoxal on Fe₂O₃ particles has not been explored, previous studies reported that glyoxal can react with Al₂O₃ particles to produce organic acid. ⁵⁹ Given that γ -Fe₂O₃ are also active particles, it is reasonable to infer that glyoxal can be adsorbed on the surface of γ -Fe₂O₃ particles and undergo further conversion. Since the amounts of S(IV) and

glyoxal are comparable to surface hydroxyl groups, the observed inhibition effect of glyoxal may be partially explained by competition of surface OH groups with S(IV). Importantly, a glyoxal molecule is released from the reaction of glyoxal—S(IV) adducts with the surface hydroxyl group, suggesting that the formation of glyoxal—S(IV) adducts in the initial step do not retard the competition between glyoxal and S(IV) due to the regeneration of glyoxal. Furthermore, we performed the reaction at a much higher ratio of glyoxal/S(IV) to surface OH groups (\sim 50) using ATR-FTIR spectroscopy. Figure 6 shows

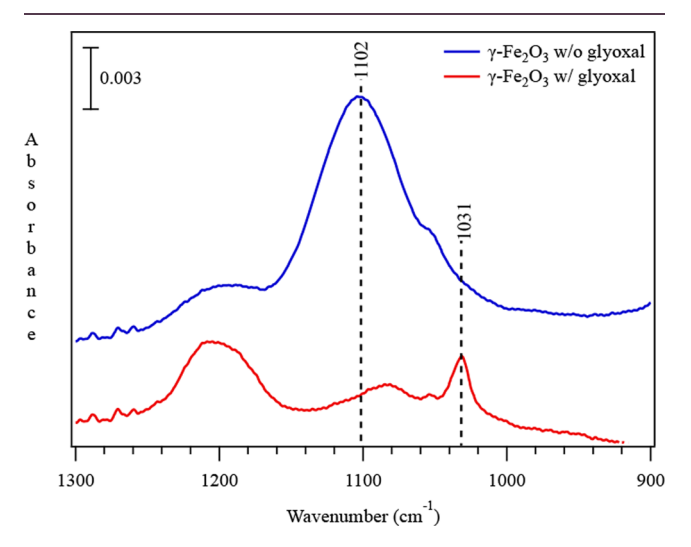


Figure 6. ATR-FTIR spectra of oxidation products from S(IV) oxidation by Fe_2O_3 particles in the presence and absence of glyoxal at pH 5. Experimental conditions: $[S(IV)]_0 = 50$ mM; [glyoxal] = 50 mM; γ -Fe₂O₃ = 1 g L⁻¹; T = 25 °C. The spectra were collected after 1 h of reaction. The band at 1102 cm⁻¹ is characteristic of aqueous-phase sulfate. Under these conditions of pH, temperature, and glyoxal concentrations the S(IV) oxidation is inhibited during the 1 h reaction time.

the spectra of the filtered solution obtained from the reaction of S(IV) with γ -Fe₂O₃ particles in the presence and absence of glyoxal. Previous studies revealed that S(IV) is capable of displacing sulfate ions from surface coordination sites after their production; ^{20,26} thus, the formed sulfate remaining on the surface of particles during solution extraction can be excluded. In the absence of glyoxal, the distinct formation of sulfate is observed with the high intensity of the band at 1102 cm⁻¹, assigned to the asymmetric stretching of sulfate, ^{26,60,61} whereas the 1102 cm⁻¹ peak is barely visible in the presence of high concentrations of glyoxal. This result indicates that the reaction is significantly inhibited under the conditions used.

4. CONCLUSION AND ATMOSPHERIC IMPLICATIONS

The present study shows that the catalytic oxidation of S(IV) can be inhibited by the presence of glyoxal. The extent of the inhibition effect depends on the concentration of glyoxal as well as solution pH. For TMI-catalyzed sulfur oxidation, this inhibition effect is proposed to arise from the trapping of SO_4^- radicals as well as the formation of glyoxal—S(IV) adducts, and the contribution of these processes depends on the ratio of S(IV) to glyoxal. Although the presence of glyoxal can slow the rate of S(IV) catalytic oxidation, the conversion of S(IV) to S(VI) does eventually occur, suggesting that the S(IV) lifetime is longer in aqueous aerosols as well as cloud and fog droplets. Additionally, with the exception of glyoxal—S(IV) adducts,

there is no observation of other organosulfur compounds formed. This observation is quite different from our previous study,³⁹ which investigated the mechanism of TMI-catalyzed S(IV) oxidation influenced by other two carbonyl compounds, namely, methacrolein (MACR) and methyl vinyl ketone (MVK), finding that various organosulfur compounds can be formed during this process. This discrepancy can be ascribed to the much faster rate of the sulfoxy radical addition reactions across the carbon–carbon double bond within MACR and MVC than the hydrogen abstraction reactions.

Additionally, we also investigated the role glyoxal plays in the reaction of S(IV) with solid iron oxide particles when the oxidation of S(IV) is dominated by heterogeneous reaction. For these particles, inhibition effects of glyoxal on sulfur oxidation is ascribed to competitive adsorption of glyoxal and sulfite with surface hydroxyl groups. Overall, our findings show that glyoxal can inhibit the oxidation of S(IV) catalyzed by aqueous Fe(III) as well as solid Fe(III), which is the most abundant transition metal in the atmospheric aqueous phase and mineral dust. 62,63 Given that the catalytic oxidation of S(IV) is an important in-cloud sulfate formation pathway, consideration of the effects of water-soluble organics such as glyoxal, as well as other carbonyl compounds, on this catalytic reaction is needed to accurately predict the formation of sulfate in the atmosphere.

ASSOCIATED CONTENT

S Supporting Information

The Supporting Information is available free of charge on the ACS Publications website at DOI: 10.1021/acsearthspace-chem.8b00168.

A table with experimental conditions; blank of reactions at different pH; first-order decay plots of $ln([S(IV)]_t/[S(IV)]_0)$ versus time; ATR-FTIR spectra of Na_2SO_3 , glyoxal and Na_2SO_3 with glyoxal (PDF)

AUTHOR INFORMATION

Corresponding Author

*E-mail: vhgrassian@ucsd.edu.

ORCID ®

Vicki H. Grassian: 0000-0001-5052-0045

Author Contributions †Co-first authors.

Notes

The authors declare no competing financial interest.

ACKNOWLEDGMENTS

This material is based upon work supported by the National Science Foundation under Grant No. AGS1702488. The authors also acknowledge the use of instruments within the Environmental Complex Analysis Laboratory located in the Department of Chemistry and Biochemistry on the Univ. of California, San Diego, campus.

REFERENCES

(1) Seinfeld, J. H.; Pandis, S. N. Atmospheric Chemistry and Physics: from air pollution to climate change, 2nd ed.; Wiley: New York, 2006. (2) Alexander, B.; Park, R. J.; Jacob, D. J.; Gong, S. Transition metal-catalyzed oxidation of atmospheric sulfur: global implications for the sulfur budget. J. Geophys. Res. 2009, 114, D02309.

- (3) Brandt, C.; Van Eldik, R. Transition metal-catalyzed oxidation of sulfur (IV) oxides. Atmospheric-relevant processes and mechanisms. *Chem. Rev.* **1995**, 95, 119–190.
- (4) Wolf, A.; Deutsch, F.; Hoffmann, P.; Ortner, H. M. The influence of oxalate on Fe-catalysed S(IV) oxidation by oxygen in aqueous solution. *J. Atmos. Chem.* **2000**, *37*, 125–135.
- (5) Podkrajsek, B.; Grgic, I.; Tursic, J.; Bercic, G. Influence of atmospheric carboxylic acids on catalytic oxidation of sulfur(IV). *J. Atmos. Chem.* **2006**, 54, 103–120.
- (6) Grgic, I.; Podkrajsek, B.; Barzaghi, P.; Herrmann, H. Scavenging of SO₄⁻ radical anions by mono- and dicarboxylic acids in the Mn(II)-catalyzed S(IV) oxidation in aqueous solution. *Atmos. Environ.* **2007**, *41*, 9187–9194.
- (7) Herrmann, H. Kinetics of aqueous phase reactions relevant for atmospheric chemistry. *Chem. Rev.* **2003**, *103* (12), 4691–4716.
- (8) Opletal, M.; Novotný, P.; Rejl, F. J.; Moucha, T.; Kordač, M. Kinetics of catalytic oxidation of sulfite in diluted aqueous solutions. *Chem. Eng. Technol.* **2015**, *38*, 1919–1924.
- (9) Clifton, C. L.; Huie, R. E. Rate constants for hydrogen abstraction reactions of the sulfate radical, SO₄-Alcohols. *Int. J. Chem. Kinet.* **1989**, *21*, 677–687.
- (10) Huie, R. E.; Clifton, C. L. Rate constants for hydrogen abstraction reactions of the sulfate radical, SO_4 ⁻Alkanes and ethers. *Int. J. Chem. Kinet.* **1989**, *21*, 611–619.
- (11) Pasiuk-Bronikowska, W.; Bronikowski, T.; Ulejczyk, M. Inhibition of the S(IV) autoxidation in the atmosphere by secondary terpenic compounds. *J. Atmos. Chem.* **2003**, *44*, 97–111.
- (12) Pasiuk-Bronikowska, W.; Bronikowski, T.; Ulejczyk, M. Synergy in the autoxidation of S(IV) inhibited by phenolic compounds. *J. Phys. Chem. A* **2003**, *107*, 1742–1748.
- (13) Ziajka, J.; Pasiuk-Bronikowska, W. Rate constants for atmospheric trace organics scavenging SO₄⁻ in the Fe-catalysed autoxidation of S(IV). *Atmos. Environ.* **2005**, *39*, 1431–1438.
- (14) Ziajka, J.; Rudzinski, K. J. Autoxidation of SIV inhibited by chlorophenols reacting with sulfate radicals. *Environ. Chem.* **2007**, *4*, 355–363.
- (15) Rudziński, K. J.; Gmachowski, L.; Kuznietsova, I. Reactions of isoprene and sulphoxy radical-anions a possible source of atmospheric organosulphites and organosulphates. *Atmos. Chem. Phys.* **2009**, *9*, 2129—2140.
- (16) Meena, V. K.; Dhayal, Y.; Rathore, D. S.; Chandel, C. P.; Gupta, K. S. Inhibition of atmospheric aqueous phase autoxidation of sulphur dioxide by volatile organic compounds: mono-, di-and trisubstituted benzenes and benzoic acids. *Prog. React. Kinet. Mech.* **2017**, *42*, 111–125.
- (17) Neta, P.; Madhavan, V.; Zemel, H.; Fessenden, R. W. Rate constants and mechanism of reaction of SO₄⁻ with aromatic compounds. J. Am. Chem. Soc. 1977, 99, 163–164.
- (18) Raber, W. H.; Moortgat, G. K. Progress and Problems in Atmospheric Chemistry; Barker, J., Ed.; World Scientific Publishing: Singapore, 1996.
- (19) Carlier, P.; Hannachi, H.; Mouvier, G. The chemistry of carbonyl compounds in the atmosphere A review. *Atmos. Environ.* **1986**, 20, 2079–2099.
- (20) Faust, B. C.; Hoffmann, M. R. Photoinduced reductive dissolution of α -Fe₂O₃ by bisulfite. *Environ. Sci. Technol.* **1986**, 20, 943–948.
- (21) Faust, B. C.; Hoffmann, M. R.; Bahnemann, D. W. Photocatalytic oxidation of sulfur dioxide in aqueous suspensions of iron oxide $(\alpha\text{-Fe}_2O_3)$. *J. Phys. Chem.* **1989**, 93, 6371–6381.
- (22) Prasad, D. S. N.; Rani, A.; Gupta, K. S. Surface-catalyzed oxidation of sulfur(IV) in aqueous silica and copper(II) oxide suspensions. *Environ. Sci. Technol.* **1992**, *26*, 1361–1368.
- (23) Ansari, A.; Peral, J.; Domenech, X.; Rodriguez-Clemente, R.; Roig, A.; Molins, E. Photo-oxidation of sulfite ions in the presence of some iron oxides. *J. Photochem. Photobiol., A* **1995**, *87*, 121–125.
- (24) Ansari, A.; Peral, J.; Domènech, X.; Rodriquez-Clemente, R. Oxidation of HSO_3^- in aqueous suspensions of α -Fe₂O₃ α FeOOH,

- β -FeOOH and γ -FeOOH in the dark and under illumination. *Environ. Pollut.* **1997**, 95, 283–288.
- (25) Gupta, K. S.; Mehta, R. K.; Sharma, A. K.; Mudgal, P. K.; Bansal, S. P. Kinetics of uninhibited and ethanol-inhibited CoO, Co₂O₃ and Ni₂O₃ catalyzed autoxidation of sulfur(IV) in alkaline medium. *Transition Met. Chem.* **2008**, 33, 809–817.
- (26) Gankanda, A.; Coddens, E. M.; Zhang, Y.; Cwiertny, D. M.; Grassian, V. H. Sulfate formation catalyzed by coal fly ash, mineral dust and iron (III) oxide: variable influence of temperature and light. *Environ. Sci.* **2016**, *18*, 1484–1491.
- (27) Atkinson, R. Atmospheric chemistry of VOCs and NOx. *Atmos. Environ.* **2000**, 34, 2063–2101.
- (28) Volkamer, R.; Platt, U.; Wirtz, K. Primary and secondary glyoxal formation from aromatics: experimental evidence for the bicycloalkyl-radical pathway from benzene, toluene, and p-xylene. *J. Phys. Chem. A* **2001**, *105*, 7865–7874.
- (29) Volkamer, R.; Molina, L. T.; Molina, M. J.; Shirley, T.; Brune, W. H. DOAS measurement of glyoxal as an indicator for fast VOC chemistry in urban air. *Geophys. Res. Lett.* **2005**, 32, L08806.
- (30) Galloway, M. M.; Huisman, A. J.; Yee, L. D.; Chan, A. W. H.; Loza, C. L.; Seinfeld, J. H.; Keutsch, F. N. Yields of oxidized volatile organic compounds during the OH radical initiated oxidation of isoprene, methyl vinyl ketone, and methacrolein under high-NOx conditions. *Atmos. Chem. Phys.* **2011**, *11*, 10779–10790.
- (31) Sander, R. Compilation of Henry's law constants (version 4.0) for water as solvent. *Atmos. Chem. Phys.* **2015**, *15*, 4399–4981.
- (32) Matsumoto, K.; Kawai, S.; Igawa, M. Dominant factors controlling concentrations of aldehydes in rain, fog, dew water, and in the gas phase. *Atmos. Environ.* **2005**, *39*, 7321–7329.
- (33) Carlton, A. G.; Turpin, B. J.; Altieri, K. E.; Seitzinger, S.; Reff, A.; Lim, H.-J.; Ervens, B. Atmospheric oxalic acid and SOA production from glyoxal: Results of aqueous photooxidation experiments. *Atmos. Environ.* **2007**, *41*, 7588–7602.
- (34) Volkamer, R.; et al. A missing sink for gas-phase glyoxal in Mexico City: formation of secondary organic aerosol. *Geophys. Res. Lett.* **2007**, 34, L19807.
- (35) Haan, D. O.; Corrigan, A. L.; Smith, K. W.; Stroik, D. R.; Turley, J. J.; Lee, F. E.; Tolbert, M. A.; Jimenez, J. L.; Cordova, K. E.; Ferrell, G. R. Secondary organic aerosol-forming reactions of glyoxal with amino acids. *Environ. Sci. Technol.* **2009**, 43, 2818–2824.
- (36) Lim, Y. B.; Tan, Y.; Perri, M. J.; Seitzinger, S. P.; Turpin, B. J. Aqueous chemistry and its role in secondary organic aerosol (SOA) formation. *Atmos. Chem. Phys.* **2010**, *10*, 10521–10539.
- (37) Herrmann, H.; Schaefer, T.; Tilgner, A.; Styler, S. A.; Weller, C.; Teich, M.; Otto, T. Tropospheric aqueous-phase chemistry: kinetics, mechanisms, and its coupling to a changing gas phase. *Chem. Rev.* **2015**, *115*, 4259–4334.
- (38) Woo, J. L.; McNeill, V. F. Simple GAMMA v1.0 a reduced model of secondary organic aerosol formation in the aqueous aerosol phase (aaSOA). *Geosci. Model Dev.* **2015**, *8*, 1821–1829.
- (39) Huang, L.; Cochran, R.; Coddens, E.; Grassian, V. H. Formation of organosulfur compounds through transition metal ion-catalyzed aqueous phase reactions. *Environ. Sci. Technol. Lett.* **2018**, *5*, 315–321.
- (40) Schaefer, T.; van Pinxteren, D.; Herrmann, H. Multiphase chemistry of glyoxal: Revised kinetics of the alkyl radical reaction with molecular oxygen and the reaction of glyoxal with OH, NO₃ and SO₄⁻ in aqueous solution. *Environ. Sci. Technol.* **2015**, *49*, 343–350.
- (41) Hoffmann, D.; Weigert, B.; Barzaghi, P.; Herrmann, H. Reactivity of poly-alcohols towards OH, NO₃ and SO₄⁻ in aqueous solution. *Phys. Chem. Chem. Phys.* **2009**, *11*, 9351–9363.
- (42) Hayon, E.; Treinin, A.; Wilf, J. Electronic spectra, photochemistry, and autoxidation mechanism of the sulfitebisulfite-pyrosulfite systems. The $\mathrm{SO}_2^-\mathrm{SO}_3^-\mathrm{SO}_4^-$ and SO_5^- radicals. *J. Am. Chem. Soc.* **1972**, 94, 47–57.
- (43) Olson, T. M.; Hoffmann, M. R. Formation kinetics, mechanism, and thermodynamics of glyoxylic acid-S(IV) adducts. *J. Phys. Chem.* **1988**, 92, 4246–4253.

- (44) Townsend, T. M.; Allanic, A.; Noonan, C.; Sodeau, J. R. Characterization of sulfurous acid, sulfite, and bisulfite aerosol systems. *J. Phys. Chem. A* **2012**, *116*, 4035–4046.
- (45) Zhang, Z. F.; Ewing, G. E. Infrared spectroscopy of SO₂ aqueous solutions. *Spectrochim. Acta, Part A* **2002**, *58*, 2105–2113.
- (46) Kaun, N.; Vellekoop, M. J.; Lendl, B. Time-resolved fourier transform infrared spectroscopy of chemical reactions in solution using a focal plane array detector. *Appl. Spectrosc.* **2006**, *60*, 1273–1278.
- (47) Olson, T. M.; Hoffmann, M. R. Kinetics, mechanism, and thermodynamics of glyoxal-S(IV) adduct formation. *J. Phys. Chem.* **1988**, 92, 533–540.
- (48) Yu, G.; Bayer, A.; Galloway, M.; Korshavn, K.; Fry, C.; Keutsch, F. Glyoxal in aqueous ammonium sulfate solutions: products, kinetics and hydration effects. *Environ. Sci. Technol.* **2011**, *45*, 6336–6342.
- (49) Ervens, B.; Volkamer, R. Glyoxal processing by aerosol multiphase chemistry: towards a kinetic modeling framework of secondary organic aerosol formation in aqueous particles. *Atmos. Chem. Phys.* **2010**, *10*, 8219–8244.
- (50) Loeffler, K. W.; Koehler, C. A.; Paul, N. M.; De Haan, D. O. Oligomer formation in evaporating aqueous glyoxal and methyl glyoxal solutions. *Environ. Sci. Technol.* **2006**, *40*, 6318–6323.
- (51) Avzianova, E.; Brooks, S. D. Raman spectroscopy of glyoxal oligomers in aqueous solutions. *Spectrochim. Acta, Part A* **2013**, *101*, 40–48.
- (52) Olson, T. M.; Hoffmann, M. R. Hydroxyalkylsulfonate formation: its role as a sulfur (IV) reservoir in atmospheric water droplets. *Atmos. Environ.* **1989**, 23, 985–97.
- (53) Rubasinghege, G.; Lentz, R. W.; Scherer, M. M.; Grassian, V. H. Simulated atmospheric processing of iron oxyhydroxide minerals at low pH: roles of particle size and acid anion in iron dissolution. *Proc. Natl. Acad. Sci. U. S. A.* **2010**, *107*, 6628–6633.
- (54) Chen, H.; Laskin, A.; Baltrusaitis, J.; Gorski, C. A.; Scherer, M. M.; Grassian, V. H. Coal fly ash as a source of iron in atmospheric dust. *Environ. Sci. Technol.* **2012**, *46*, 2112–2120.
- (55) Jacob, D. J.; Gottlieb, E. W.; Prather, M. J. Chemistry of a polluted cloudy boundary layer. *J. Geophys. Res.* **1989**, *94*, 12975–13002.
- (56) Martin, L. R.; Easton, M. P.; Foster, J. W.; Hill, M. W. Oxidation of hydroxymethanesulfonic acid by Fenton's reagent. *Atmos. Environ.* **1989**, 23, 563–568.
- (57) Olson, T. M.; Fessenden, R. W. Pulse radiolysis study of the reaction of OH radicals with methanesulfonate and hydroxymethanesulfonate. *J. Phys. Chem.* **1992**, *96*, 3317–3320.
- (58) Huie, R. E.; Neta, P. Rate constants for some oxidations of S(IV) by radicals in aqueous solutions. *Atmos. Environ.* **1987**, 21, 1743–1747.
- (59) Shen, X. L.; Wu, H. H.; Zhao, Y.; Huang, D.; Huang, L. B.; Chen, Z. M. Heterogeneous reactions of glyoxal on mineral particles: A new avenue for oligomers and organosulfate formation. *Atmos. Environ.* **2016**, *131*, 133–140.
- (60) Hug, S. J. In Situ Fourier transform infrared measurements of sulfate adsorption on hematite in aqueous solutions. *J. Colloid Interface Sci.* **1997**, *188*, 415–422.
- (61) Liu, C.; Ma, Q.; Liu, Y.; Ma, J.; He, H. Synergistic reaction between SO₂ and NO₂ on mineral oxides: a potential formation pathway of sulfate aerosol. *Phys. Chem. Chem. Phys.* **2012**, *14*, 1668–1676.
- (62) Deguillaume, L.; Leriche, M.; Desboeufs, K.; Mailhot, G.; George, C.; Chaumerliac, N. Transition metals in atmospheric liquid phases: sources, reactivity, and sensitive parameters. *Chem. Rev.* **2005**, 105, 3388–3431.
- (63) Zhang, Y.; Mahowald, N.; Scanza, R. A.; Journet, E.; Desboeufs, K.; Albani, S.; Kok, J. F.; Zhuang, G.; Chen, Y.; Cohen, D. D.; Paytan, A.; Patey, M. D.; Achterberg, E. P.; Engelbrecht, J. P.; Fomba, K. W. Modeling the global emission, transport and deposition of trace elements associated with mineral dust. *Biogeosciences* **2015**, *12*, 5771–5792.